

Particle creation via high frequency dispersion

Steven Corley*

Department of Physics, University of Maryland, College Park, Maryland 20742-4111

(Received 7 October 1996; revised manuscript received 17 December 1996)

We investigate the particle creation caused by a nonlinear dispersion relation for a massless scalar field propagating on a background curved spacetime in two dimensions. The dispersion relation adopted agrees with the standard dispersion relation at long wavelengths but is modified at short wavelengths, the division being characterized by a new length scale $1/k_0$. We consider both spacetimes with and without a black hole. Those without contain instead a uniformly moving ‘‘bump.’’ The black hole cases considered have Hawking temperatures $T_H > k_0/100$. We find that the particle creation arises in all cases from two effects: *scattering and mode conversion*. The latter was identified by Corley and Jacobson as the phenomenon responsible for the Hawking effect. [S0556-2821(97)04910-2]

PACS number(s): 04.70.Dy, 04.60.Kz, 04.62.+v

I. INTRODUCTION

In an effort to understand the role of high frequencies in derivations of the Hawking effect, see, for instance, [2,3], Unruh studied the particle creation for a quantum scalar field satisfying a wave equation with high frequency dispersion and propagating on a black hole spacetime,¹ see [4]. Further investigations of similar models were considered by Brout, Massar, Parentani, and Spindel [6], and by Corley and Jacobson [1]. In [1] it was realized that the particle creation in such models comes from two sources. The expected Hawking particles are produced by a phenomenon known as mode conversion, in this case a high frequency, ingoing wave packet is converted into a low frequency, outgoing wave packet with the same sign wave vector. The second source of particle creation is scattering.

The fact that particle creation could occur by scattering is hardly surprising. The quantum state of the field was taken to be the freefall vacuum, that is, the state annihilated by annihilation operators for positive freefall frequency modes. However, the particles were measured relative to the Killing vacuum at infinity. Similar types of particle creation occur elsewhere; for instance, in de Sitter spacetime. What makes the result somewhat surprising in this case is that it does not occur with the standard wave equation.

In this paper we further investigate the particle creation caused by scattering for a class of metrics containing a ‘‘spacetime bump,’’ but *no* black hole, moving uniformly relative to an asymptotic freefall observer. The source of the bump could be, for instance, a cosmic string traveling through space. We find that scattering in such spacetimes is

not the only source of particle creation, but rather that mode conversion is also important, even when no black hole is present. Roughly, the low frequency particle creation arises from scattering only, whereas the high frequency particle creation arises from both scattering and mode conversion. Essentially mode conversion does not turn on until a critical frequency is reached. This frequency is determined by the speed of a freefall observer passing through the bump. The larger the speed, the smaller the critical frequency until it reaches zero when the bump becomes a black hole.

We also extend the analysis of [1] to high temperature black holes. Although we do not expect our model to be a good approximation to physics in the presence of such a black hole, it nevertheless is of interest for the following reason. We expect our model to predict a particle flux very different from the thermal Hawking spectra (at all frequencies) for a high temperature black hole (in contrast to a black hole with $T_H \ll k_0$). We show that this is indeed the case by considering a few black hole spacetimes all having a Hawking temperature $T_H > k_0/100$. We find that the ‘‘transition temperature’’ where the entire particle spectrum begins to deviate from the thermal prediction occurs roughly around $k_0/100$.

This paper is organized as follows. In Secs. II and III we very briefly introduce the model for the scalar field and discuss the method employed to compute the particle creation, the details have been given in [1]. In Sec. IV we present the results of the computations. In Sec. V we discuss the results and in Sec. VI we make some concluding remarks. We use units where $c = \hbar = 1$.

II. THE MODEL AND ITS QUANTIZATION

We adopt the following equation of motion for the scalar field:

$$(\partial_t + \partial_x v)(\partial_t + v \partial_x) \phi = \partial_x^2 \phi + \frac{1}{k_0^2} \partial_x^4 \phi. \quad (1)$$

If we throw away the fourth derivative term, we recover the standard wave equation in the curved spacetime metric:

*Electronic address: corley@umdhep.umd.edu

¹Actually he motivated the modified wave equation by considering the sonic hole analogue [5], in which one looks at fluid perturbations about an irrotational background flow. In this case, small perturbations may be described using an effective scalar field theory. The dispersion relation for such a field is modified at short wavelengths (in the frame of the background flow) due to finite size effects of the atoms. From the sonic-hole–black-hole analogy, this may be immediately mapped to the black hole case.

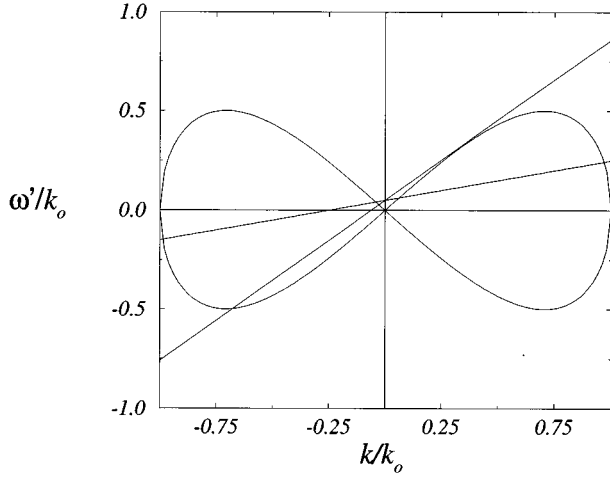


FIG. 1. Plot of the curved spacetime dispersion relation for two different values of $v(x)$. The intersection points of the two curves are the mode solutions to the wave equation when $v(x) = \text{constant}$. From left to right we label the wave vectors as k_{-l} , k_{-s} , k_{+s} , and k_{+l} . For the larger slope straight line, the k_{+s} and k_{+l} have become degenerate.

$$ds^2 = dt^2 - [dx - v(x)dt]^2. \quad (2)$$

This metric is a generalization of the Schwarzschild metric written in Lemaitre coordinates. We follow the convention that $v(x) < 0$. If $v(x)$ becomes less than -1 somewhere, we have a black hole spacetime with horizon at $v(x) = -1$.

The dispersion relation for Eq. (1) is given by

$$[\omega - v(x)k]^2 = k^2 \left[1 - \left(\frac{k}{k_0} \right)^2 \right], \quad (3)$$

where we define

$$\omega' = \omega - v(x)k. \quad (4)$$

We refer to ω' as the freefall frequency as it is the frequency measured by a freefall observer in the above metric. A plot of the dispersion relation in the freefall frame is shown in Fig. 1. The curved line corresponds to the square root of the right-hand side of Eq. (3), while the straight line is the freefall frequency (4). The intersection points are the allowed wave vectors for the given ω . In increasing order of their values, we shall refer to them as k_{-l} , k_{-s} , k_{+s} , and k_{+l} . The $+/-$ subscript refers to the sign of the wave vector and the s/l subscript to its magnitude, “small” or “large,” respectively. Furthermore, for a given value of $v(x)$, there is a corresponding value of ω such that $k_{+s} = k_{+l}$ (an example is shown in Fig. 1). We refer to this value as $\omega_{\text{crit}}[v(x)]$. If $\omega > \omega_{\text{crit}}(v_1)$ and $v(x) = v_1$, then k_{+s} and k_{+l} become complex conjugates, while k_{-s} and k_{-l} remain real.

Quantization of this model is carried out in [1], so we shall not repeat the details. However, an important property we shall need later is the following. There are two natural sets of positive norm modes used in a normal mode decomposition of the field. The first are positive Killing frequency modes which are defined by the Killing frame observers located at infinity who measure the particle creation. The second are positive freefall frequency modes which are defined

by the freefall observers located at $x \gg 0$. We take the ground state of the theory to be the state annihilated by positive freefall frequency annihilation operators.

Before ending this section, we introduce the background geometries [$v(x)$'s] that we shall study. There are two classes that we shall consider. The first are given by

$$v_b(x) = v_0 + \frac{v_0 - v_1}{2} \left[\text{sgn}(x - a/2) \left(\frac{\tanh(\kappa|x - a/2|)^\delta}{\tanh(\kappa a/2)^\delta} \right)^{1/\delta} - \text{sgn}(x + a/2) \left(\frac{\tanh(\kappa|x + a/2|)^\delta}{\tanh(\kappa a/2)^\delta} \right)^{1/\delta} \right] \quad (5)$$

and the second by

$$v_{\text{BH}}(x) = \frac{v_0 + v_1}{2} + \frac{v_0 - v_1}{2} \text{sgn}(x) [\tanh(\kappa|x|)^\delta]^{1/\delta}. \quad (6)$$

They are characterized by the real, constant parameters v_0 , v_1 , κ , and δ , and $v_b(x)$ also contains the free parameter a . We shall always² take $v_0 = -0.5$, although the results are not independent of this, the general features that we shall describe are. We shall also always take $-1 < v_1 < v_0 < 0$ for the $v_b(x)$ metrics and $v_1 < -1$ for the $v_{\text{BH}}(x)$ metrics. The first class describes smoothed out spacetime bumps and the second black holes. In both cases the parameter κ controls the maximum value of the derivative of $v(x)$ and δ controls the sharpness of the transition regions. For the first class, the parameter a controls the width of the spacetime bump. In the limit $\kappa \rightarrow \infty$, $v_{\text{BH}}(x)$ reduces to v_0 for positive x and v_1 for negative x . Similarly, $v_b(x)$ reduces to v_1 for $-a/2 < x < a/2$ and v_0 otherwise. Hence, in this limit both the bump and black hole metrics contain discontinuities. All of these geometries are static, but relative to the freefall frame at $x \gg +\infty$ the bump and/or black hole is moving to the right at speed v_0 .

III. SOLVING THE EQUATION OF MOTION

Our goal is to compute the particle production resulting from the scattering of vacuum fluctuations off the background geometry. This requires in one way or another solving Eq. (1). By choosing to work with fixed Killing frequency solutions only [that is, solutions of the form $e^{-i\omega t} f(x)$], we can reduce the problem to solving the ordinary differential equation (ODE)

$$(-i\omega + \partial_x v)(-i\omega + v \partial_x) f(x) = \left(\partial_x^2 + \frac{1}{k_0^2} \partial_x^4 \right) f(x). \quad (7)$$

However, this requires boundary conditions. In the time dependent picture the appropriate boundary conditions are that one has at late times a positive Killing frequency, right-moving wave packet located at $x \gg 0$. We would like the corresponding boundary conditions for the ODE. We now discuss these conditions.

²We would like to take $v_0 = 0$; however, our wave equation appears to break down in this limit. This is discussed in detail in [1] and [7].

In the bump background geometry, $v_b(x) \approx v_0$ for $x \gg 0$ or $x \ll 0$. In these regions Eq. (1) possesses wave packet solutions composed of modes $e^{-i[\omega t - k(\omega)x]}$. The wave vector $k(\omega)$ is a root of the curved spacetime dispersion relation.³ These wave packets travel at a group velocity

$$v_g \equiv \frac{d\omega}{dk} \quad (8)$$

relative to a Killing observer. Using this one may show that the k_{+s} wave vector produces right-moving wave packets, and the k_{-l} , k_{-s} , and k_{+l} wave vectors produce left-moving wave packets. Therefore, in order to have only a right-moving wave packet in the $x \gg 0$ region at late time, we must only ever have a right-moving wave packet in the $x \ll 0$ region. Hence, our boundary condition is that the solution becomes $e^{ik_{+s}x}$ as $x \rightarrow -\infty$.

The relevant boundary condition for black hole geometries was discussed in [1]. It was shown there that the relevant mode solution grows exponentially with increasing x inside the horizon, and, in fact, that the solution outside the horizon is quite insensitive (up to an overall scale factor) to the boundary condition.

Given the above boundary conditions, the equation can now be solved numerically,⁴ or in the special case where $\kappa \rightarrow \infty$, exactly, for either metric. With the solution in hand, it is a simple matter to compute the number expectation value for wave packets narrowly peaked about a given Killing frequency. The relevant expressions along with derivations can be found in [1].

IV. RESULTS

A. Bump

We begin by describing the results of the exactly solvable cases. In Fig. 2 we plot the number expectation value as a function of frequency for $ak_0 = 1, 2, 3, 5, 7, \text{ and } 9$, where $\kappa = \infty$ and $v_1 = -0.9$ in all cases. The maxima of the curves move toward smaller ω with increasing a (for $ak_0 = 9$ we refer to the leftmost local maximum). The respective luminosities are $0.00021k_0^2$, $0.00044k_0^2$, $0.00048k_0^2$, $0.00027k_0^2$, $0.00021k_0^2$, and $0.00022k_0^2$. Because of the natural scale $1/k_0$ in the problem, we expect different particle spectra for the extreme limits $ak_0 \ll 1$ and $ak_0 \gg 1$. This graph illustrates exactly this point (we have plotted only $ak_0 \approx 1$ since the $ak_0 \ll 1$ case is qualitatively the same).

A further increase in ak_0 produces a particle number spectra as in Fig. 3. The parameters in this case are $ak_0 = 50$, $v_1 = -0.9$, and $\kappa = \infty$. The luminosity for this case is $0.00024k_0^2$. If we further increase a , more oscillations appear over the same frequency range. However, the spectrum above $\omega \approx 0.0165$ remains almost exactly the same. Furthermore, we note that varying v_0 and v_1 leaves the qualitative features unchanged.

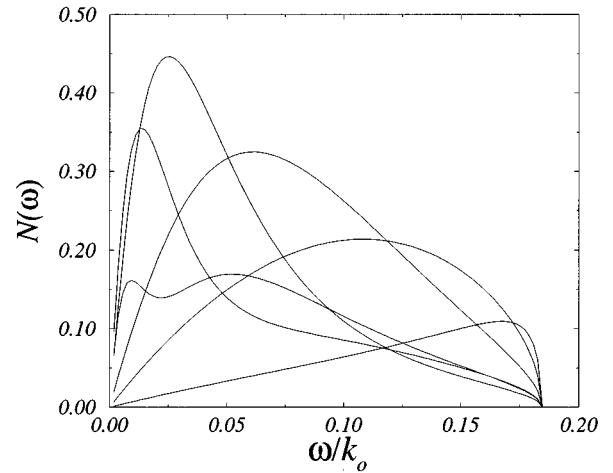


FIG. 2. Number expectation value as a function of Killing frequency for the bump metric. The parameter sets are $v_1 = -0.9$, $\kappa = \infty$, and $ak_0 = 1, 2, 3, 5, 7, \text{ and } 9$. The peaks (leftmost for $ak_0 = 9$) move towards decreasing ω as ak_0 increases.

For finite κ the results are qualitatively the same. We illustrate this for two cases. In Fig. 4 we plot the number expectation value for the two parameter sets $\kappa = k_0/10$ and k_0 (larger κ produces more particles). The other parameters are $ak_0 = 1$, $v_1 = -0.9$, and $\delta = 5$ in both cases. The respective luminosities are $0.000021k_0^2$ and $0.00037k_0^2$. Because of the finite κ , the length of the bump is not given by a . We instead define an effective length as the distance between the two $v_b(x) = -0.7$ locations. We obtain approximate values of $2/k_0$ for the $\kappa = k_0$ case and $20/k_0$ for the $\kappa = k_0/10$ case. The relevance of this length is that it seems to determine the frequency of oscillation in the spectrum. This is evident after comparing the $\kappa = \infty$, $ak_0 = 2$ metric spectrum in Fig. 2 with the $\kappa = k_0$ metric spectrum of Fig. 4. A similar comparison of the $\kappa = k_0/10$ metric spectrum of Fig. 4 with that of the $\kappa = \infty$, $ak_0 = 20$ metric spectrum (not shown) also agrees with this.

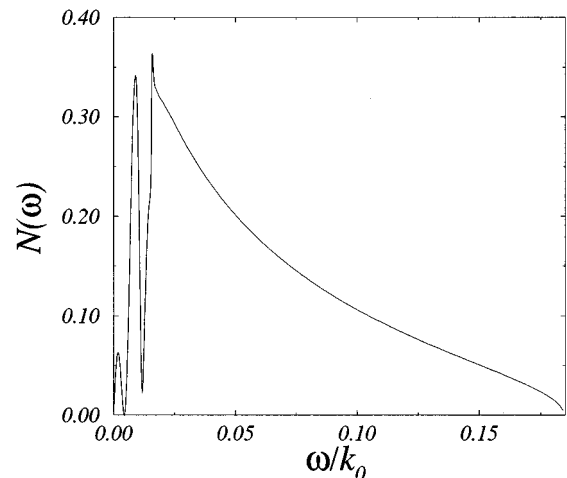


FIG. 3. Number expectation value as a function of Killing frequency for the bump metric. The parameter set is $v_1 = -0.9$, $\kappa = \infty$, and $ak_0 = 50$.

³We consider only frequencies ω such that all roots to the dispersion relation are real for the given value of v_0 .

⁴We used MATHEMATICA to solve Eq. (7).

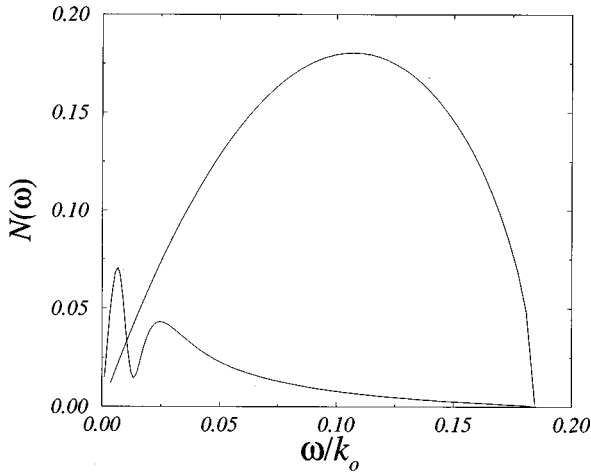


FIG. 4. Number expectation value as a function of Killing frequency for the bump metric. The parameter sets are $ak_0=1$, $v_1=-0.9$, $\delta=5$, and $\kappa=k_0/10$ and k_0 . The larger κ produces more particles.

For the other finite κ parameters, we shall just summarize the qualitative features of the spectra. We define as above an effective length a_{eff} as the distance between the two locations where $v_b(x)=(v_0+v_1)/2$. When $a\kappa \gg 1$ and $\delta \gg 1$, $a_{\text{eff}} \approx a$; otherwise we have $a_{\text{eff}} > a$. We find that the shape of the particle flux spectrum is qualitatively that of the $\kappa = \infty$ bump metric with the same v_0 and v_1 and with length a_{eff} . That is, the number of oscillations is the same, and their respective peaks occur at approximately the same frequencies. They differ in the amount of particle creation though. If $\kappa/k_0 \gg 1$, $a\kappa \gg 1$, and $\delta \gg 1$ this difference is fairly small; otherwise, the amount of particle creation for the smoothed out bump metrics is significantly smaller.

To see the behavior of the amount of particle creation, we plot in Fig. 5 the luminosity as a function of bump length a for the $\kappa = \infty$ bump metrics with $v_1 = -0.9$. The luminosity starts oscillating with a large amplitude until the bump reaches a sufficient length ($ak_0 \gg 1$). After that it continues to oscillate about a fixed luminosity with a much smaller

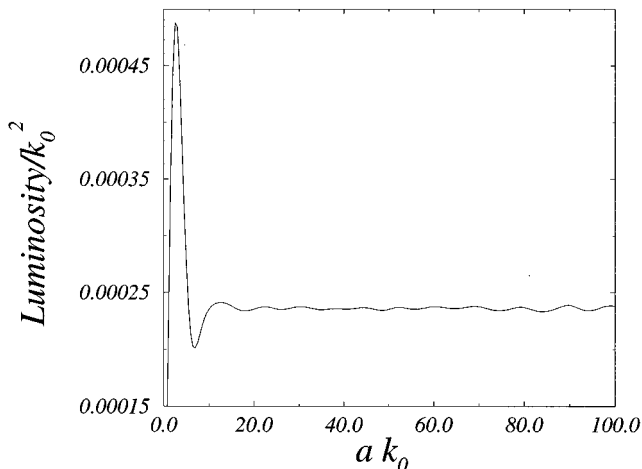


FIG. 5. Plot of the luminosity for the bump metric with $\kappa = \infty$ and $v_1 = -0.9$ as a function of the bump length ak_0 .

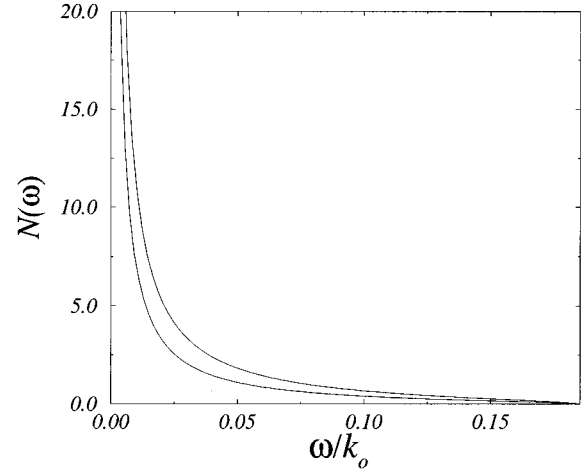


FIG. 6. Number expectation value as a function of Killing frequency for the black hole metrics. The parameter sets are $\kappa = \infty$, and $v_1 = -1.25$ and -1.5 . The larger amplitude curve corresponds to the larger $|v_1|$.

amplitude of oscillation. We see a similar behavior of the luminosity as the other parameters (v_1, v_0, κ, δ) are varied.

B. High temperature black holes

We again begin with the exactly solvable cases. In Fig. 6 we plot the number expectation value versus frequency for the black hole metrics with parameter sets $\kappa = \infty$, and $v_1 = -1.25$ and -1.5 (larger $|v_1|$ produces more particles). The respective luminosities are $0.00123k_0^2$ and $0.00202k_0^2$. If we further increase $|v_1|$, the particle creation per Killing frequency increases. However it does not increase without bound with increasing $|v_1|$, but rather asymptotes to an upper bound.

We are also interested in large, but finite, temperature black holes. In Fig. 7 we plot the numerically generated number expectation value for a pair of black hole metrics and the corresponding thermal prediction for each. In increasing order of the amount of particle creation the curves are a black hole metric with $T_H = k_0/5$, a black hole metric with $T_H = k_0$, the thermal prediction for $T_H = k_0/5$, and the thermal prediction for $T_H = k_0$. For the black hole metrics the other parameters were set to $v_1 = -1.5$ and $\delta = 1$. If we further increase the temperature of the black hole metrics we find very little change in the number expectation value, while the thermal prediction increases without bound. In fact, there is less than a percent difference between the $v_1 = -1.5$ curve of Fig. 6 and the $T_H = k_0$ black hole metric of Fig. 7.

If we instead decrease the black hole temperature, we find that the numerically calculated number expectation value and the thermal prediction begin converging. For instance, keeping all the parameters for the black hole metric as above, but lowering the temperature to $T_H = k_0/10$, we find that the deviation from the thermal prediction for a black hole of the same temperature remains less than roughly 30% out to $\omega \approx 1/2T_H$. In [1] even lower temperature black holes were considered. In one case for a black hole of temperature $T_H \approx 0.0008k_0$, they found that the percent difference between the computed and thermal number expectation values

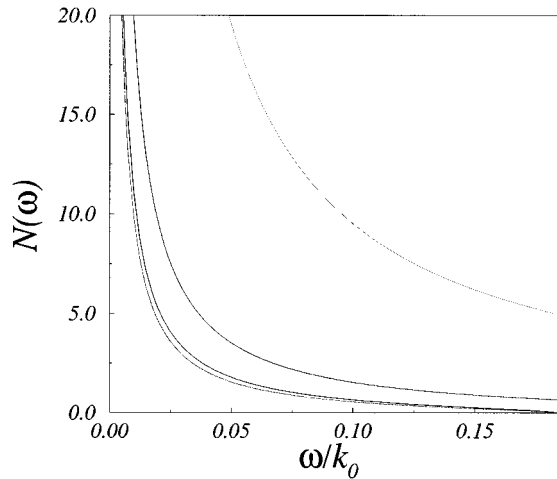


FIG. 7. Number expectation value as a function of Killing frequency for black hole metrics with temperatures $T_H = k_0$ and $T_H = k_0/5$, along with the thermal predictions for the respective temperatures. The other parameters for the black hole metrics are $v_1 = -1.5$ and $\delta = 1$. In increasing order of the amount of particle creation, the curves correspond to the lower temperature black hole metric, higher temperature black hole metric, lower temperature thermal prediction, and higher temperature thermal prediction.

remained less than 0.1% for frequencies $\omega < 43T_H$.

V. DISCUSSION

A. Bump

We begin by discussing qualitatively the source of the particle creation. We start with the $\kappa = \infty$ bump metrics, where $v_b(x) = v_1$ for $-a/2 < x < a/2$, and is v_0 otherwise. The standard method of computing the particle creation of a positive Killing frequency packet, which we take to be right moving and located at $x \gg 0$ in this case, involves propagating it backward in time. To describe this motion in words is complicated, but with a picture the qualitative features are obvious. In Fig. 8 we display the motion of such a packet. One sees that scattering occurs at $x = \pm a/2$, and results in an infinite number of left moving packets located at $x \gg 0$ and an infinite number of right moving packets located at $x \ll 0$. The packets at $x \ll 0$ are composed of purely positive freefall frequencies, but the ones at $x \gg 0$ contain both positive and negative freefall frequencies. The negative freefall frequency packets give rise to particle creation, the amount of which is proportional to the norm of their sum. The support of these packets will overlap if they are sufficiently spread out in space (which will be the case if the original right moving packet is narrowly peaked in frequency). Furthermore, it is clear that any two packets are phase shifted from one another by an amount proportional to $a\omega$ (up to an additive constant),⁵ arising from one packet propagating an extra distance proportional to a . Therefore, the cross terms in the norm of the net negative freefall frequency packet are non-

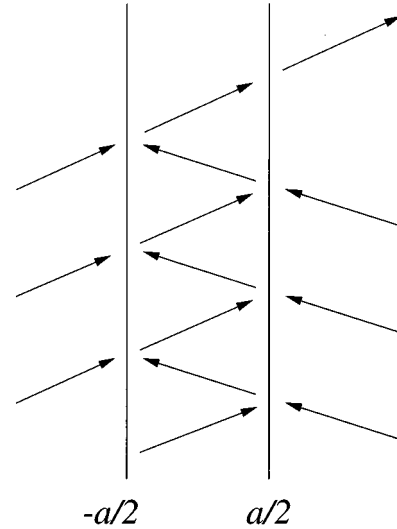


FIG. 8. Diagram of the wave packets produced by scattering when an outgoing wave packet at $x \gg 0$ is propagated backward in time. The rightward pointing arrow at $x > a/2$ is the outgoing wave packet. The leftward pointing arrows at $x > a/2$ and the rightward pointing arrows at $x < -a/2$ are the resulting ingoing packets. The former contain a negative freefall frequency part which gives rise to the particle creation.

zero, and oscillate with ω with a “frequency” proportional to a . In Fig. 3 we saw such an oscillation, and it was noted there that the number of oscillations increased as a was increased, in agreement with our findings here.

What happens when κ is finite? Qualitatively nothing changes. A new length scale, $1/\kappa$, enters the problem, which would seem to make the oscillation more complicated, but we nevertheless observe (for the few cases that we have looked at) that the “frequency” of spectrum oscillations is proportional to a_{eff} (defined in the results section). That is to say, if we consider a bump metric with $\kappa = \infty$ and $a = a_{\text{eff}}$, we get approximately the same frequency of oscillations in the spectrum as with a finite κ bump metric with effective length a_{eff} .

So far we have had to assume that the wave vector roots to the dispersion relation (3) are real in the $v_b(x) = v_1$ region. This is only true if $\omega < \omega_{\text{crit}}(v_1)$, see Sec. II. When $\omega > \omega_{\text{crit}}(v_1)$ and $v_b(x) = v_1$, two of the wave vector roots are real and the other two complex conjugates, i.e., see Sec. II. A positive Killing frequency packet centered about a frequency $\omega > \omega_{\text{crit}}(v_1)$ (and is right moving and located somewhere at $x \gg 0$) behaves very differently when propagated backward in time. For the general bump metric, i.e., κ finite, a piece of this packet will be reflected and will propagate back out toward $x = \infty$ as before (it also contains both positive and negative freefall frequencies). However, the remainder of the packet continues to propagate toward smaller x until it reaches a point where its group velocity vanishes, i.e., a classical turning point. Around this point the packet undergoes a process known as mode conversion, and turns around and propagates out toward $x = \infty$ in the form of a packet containing both positive and negative freefall frequencies.

Mode conversion, as the name implies, is a process whereby one type of mode(s) is converted into another type

⁵Actually each packet also picks up a phase from scattering, but that is proportional to ω/k_0 and is negligible compared to $a\omega$ when $a \gg 1/k_0$.

of mode(s). In this case, a right moving mode has been converted into a pair of left moving, shorter wavelength modes. This sounds like an ordinary reflection process, but it differs in one way. The sign of the wave vector of the right moving packet is the same as that of one of the left moving packets. What makes this particularly interesting is that exactly this behavior was discovered by Unruh [4] in the case of a background black hole geometry.

How can this same behavior then appear without a black hole present? The answer is that the role of the event horizon as a causal horizon has been replaced by that of an *effective horizon*. The equation of motion (1) of the field is not Lorentz invariant and the propagation of wave packets is not causal in the background metric. Nevertheless, wave packets peaked in frequency about an $\omega > \omega_{\text{crit}}(v_1)$ have a vanishing group velocity at some spatial coordinate, i.e., a classical turning point. Beyond this point the wave packet is no longer propagating, but rather tunneling. The classical turning point therefore is a sort of effective horizon, and is the place around which mode conversion occurs, in both spacetimes with and without black holes. In fact, the only special property of the event horizon in these models is that it is the infimum of positions of all effective horizons, i.e., the effective horizon for any wave packet occurs at an $|v(x)| < 1$.

What is not clear, however, is how the amount of particle creation depends on the effective horizon versus the event horizon for a black hole spacetime. This will be discussed a little more in the next section.

Above we said that a piece of a wave packet that reaches its effective horizon will tunnel through the bump. When $a \approx 1/k_0$ or smaller, this is important; however, when $a \gg 1/k_0$ and $a \gg 1/\kappa$, this effect is negligible. This implies that the number expectation value spectrum above $\omega_{\text{crit}}(v_1)$ becomes independent of a for large a . This explains why the luminosity in Fig. 5 settled down to approximately a constant value (up to a small oscillation) for large enough a .

Finally, recall that even in the $\omega > \omega_{\text{crit}}(v_1)$ case just discussed, there were multiple negative freefall frequency packets produced. Just as in the $\omega < \omega_{\text{crit}}(v_1)$ case, these packets should interfere and produce oscillations in the number expectation value spectrum. Indeed this is the case. This same behavior was noted, and discussed in detail, in [1].

B. High temperature black holes

We now turn to a discussion of high temperature black holes. These are unphysical because we do not expect physics to be described in the manner we are using at such large Hawking temperatures. However, they are of interest in the context of understanding the behavior of the modified wave equation that we have adopted as our model. Specifically we would like to know where the spectrum begins to deviate from the thermal prediction for all frequencies. For example, for the lower temperature black holes considered in [1], large deviations from thermality were found at frequencies $\omega \gg T_H$ while the low frequency spectrum was within at least $(T_H/k_0)^3$ of the thermal prediction for $\omega \leq T_H$ for certain metrics [1].

The first step is to make sure that there is a black hole whose spectrum differs significantly at all frequencies from the thermal prediction. Since we expect this to occur for high

temperature black holes, we take the limit $T_H \rightarrow \infty$. The number expectation value for such a case was plotted in Fig. 6. One can also show analytically that the low frequency spectrum is given by T_{eff}/ω to leading order in ω , where

$$T_{\text{eff}} = k_0 \sqrt{1 - v_0^2} \frac{1 + v_0}{1 - v_0} \frac{v_1 + 1}{v_1 - 1} \frac{v_1 + v_0}{v_1 - v_0}. \quad (9)$$

Since the thermal prediction is an infinite number expectation value for all frequencies, we have an example where the two predictions are very different for all frequencies. One might worry that the frequency where the two number expectation values begin to deviate significantly simply decreases with increasing Hawking temperature, converging to zero as $T_H \rightarrow \infty$. This is unlikely though. If we smooth out the black hole of Fig. 6, but still keep $\kappa \gg k_0$, we expect essentially the same number expectation value spectrum. The reason is that all the modes that enter the problem have a wavelength $> 2\pi/k_0$. Therefore, to them the background appears just as in the infinite Hawking temperature black hole. One can check this by numerical calculation also, and indeed one finds almost identical spectra under the above conditions, see, for instance, Fig. 7.

Where do the modified wave equation and the standard wave equation begin to predict the same Hawking spectra? For instance, when do their predictions differ by less than 1% at $\omega = T_H$? From dimensional analysis we would expect the transition to occur around $T_H \approx 1/k_0$. From Fig. 7 we see that this is roughly correct. As stated in the text, for a black hole with $T_H = k_0/10$ the numerical and thermal expectation number values differed by less than 30% for $\omega < T_H/2$. At $T_H = k_0/100$ the relative difference is less than 0.2% for all frequencies $\omega < T_H$. Therefore the transition occurs roughly around $T_H \approx k_0/100$. We have considered only ‘‘smoothed’’ out metrics to produce the above data, that is metrics with $\delta = 1$ or 2. The agreement gets worse as we increase δ though and hence the ‘‘transition’’ temperature would decrease.

VI. CONCLUSION

We have studied the particle creation occurring in spacetimes containing a uniformly moving bump. Qualitatively we have been able to understand the cause of the particle creation, either purely by scattering of wave packets or also by mode conversion, and the basic shape of the corresponding spectrum, i.e., the oscillations. We have also briefly considered some high temperature black holes to probe the behavior of the modified wave equation. We have shown that a transition in the number expectation value spectrum occurs around $T_H \approx k_0/100$. At smaller temperatures, the lower part of the spectrum agrees rather well [1,4,6], with the thermal prediction. At larger temperatures however, the entire spectrum deviates significantly from the thermal prediction.

Unfortunately we are still lacking more quantitative predictions. For instance, we would like to understand how the luminosity for the class of bump metrics considered scales with the various parameters, i.e., v_0 , v_1 , κ , and a . Furthermore, we would like a better estimate of the frequency of oscillations in the spectrum. However, even a very rough

calculation is a formidable task in these models. For instance, just computing the wave vector roots of the dispersion relation in some reasonable approximation when $\omega \approx k_0$ is difficult.

We are also still lacking a good understanding of what determines the amount of particle creation by mode conversion. For instance, what is the relationship between the amount of particle creation via mode conversion in a non-black-hole spacetime as compared to a black hole spacetime? Conversely we can ask what is so special about the event horizon of a black hole for our modified wave equation?

We end with two applications of this work. One possible source of the curvature making up the bump metric is a uniformly moving cosmic string. The above analysis gives an estimate, for a few cases anyway, of the amount of particles produced from its motion. Another source is to consider the

fluid flow analogue developed by Unruh [4]. Here the bump is easily generated as a spatial gradient in the flow velocity of a fluid. This would present a possibly realistic place to measure the particle creation by a mode conversion process. Obviously the sonic hole case is the most interesting, but as the above analysis shows, a sonic hole is not needed in order to create particles by mode conversion.

ACKNOWLEDGMENTS

I would like to thank the University of Utrecht, where much of this work was done, for their hospitality. I would also especially like to thank Ted Jacobson for many helpful criticisms. This work was supported by the University of Maryland.

-
- [1] S. Corley and T. Jacobson, *Phys. Rev. D* **54**, 1568 (1996).
[2] S. W. Hawking, *Nature (London)* **248**, 30 (1974); *Commun. Math. Phys.* **43**, 199 (1975).
[3] K. Fredenhagen and R. Haag, *Commun. Math. Phys.* **127**, 273 (1990).

- [4] W. G. Unruh, *Phys. Rev. D* **51**, 2827 (1995).
[5] W. G. Unruh, *Phys. Rev. Lett.* **46**, 1351 (1981).
[6] R. Brout, S. Massar, R. Parentani, and Ph. Spindel, *Phys. Rev. D* **52**, 4559 (1995).
[7] T. Jacobson, *Phys. Rev. D* **53**, 7082 (1996).